Table S1. Pore size statistics of HPHG

	Size of holes		
	Macropore(nm)	micropore(nm)	nanopore(nm)
0ZIF-8	$2.0\times10^5 \pm 6300$	4385 ± 823	195 ± 76
0.1ZIF-8	$1.8\times10^5 \pm 3900$	3258 ± 638	125 ± 48
0.3ZIF-8	$1.3\times10^5 \pm 3700$	2048 ± 546	68 ± 37
1ZIF-8	$1.2\times10^5 \pm 2900$	1845 ± 398	48 ± 28

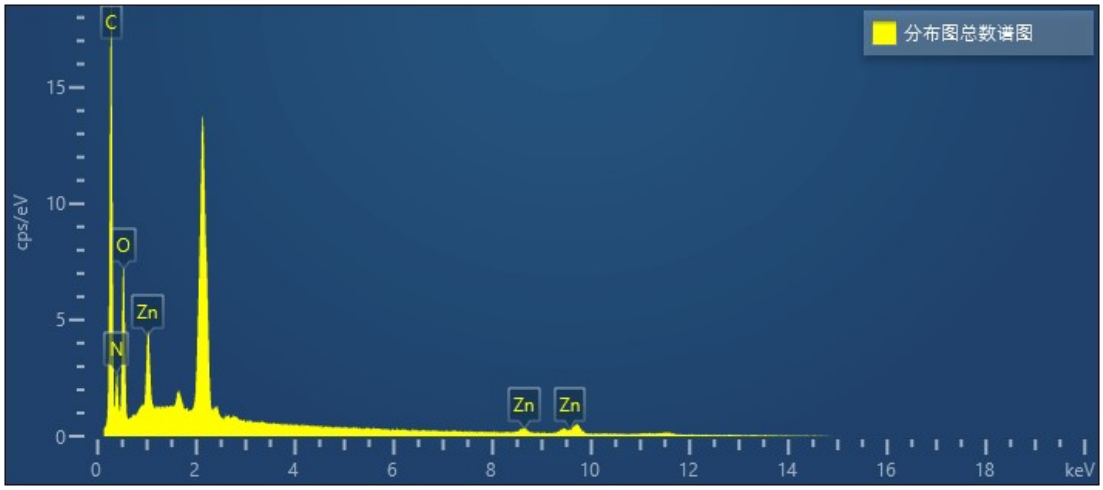

Figure S1. EDS element distribution curve.

Table S2. Element distribution statistics of HPHG.

Element	**Line type**	**wt%**	**Wt % Sigma**	**At%**
C	K	49.06	0.46	57.03
N	K	20.38	0.62	20.31
O	K	24.46	0.33	21.35
Z_n	L	6.09	0.15	1.30
Total		100.00		100.00

Table S3. BET data statistics of HPHG.

Concentration	**BET Surface Area(m^2/g)**	**BJH Adsorption cumulative volume of pores (cm^3/g)**	**Pore Size(nm)**
0.1ZIF-8	1.5415	0.020492	70.5409
0.2ZIF-8	1.0655	0.020492	77.6511
0.3ZIF-8	2.5315	0.029163	71.6100
0.5ZIF-8	4.3896	0.003996	5.9499
1.0ZIF-8	1.8699	0.002570	6.8688

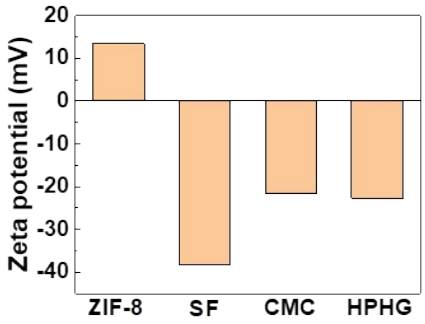

Figure S2. Zeta potential of ZIF-8 aqueous, SF aqueous, CMC aqueous and HPHG precursor.

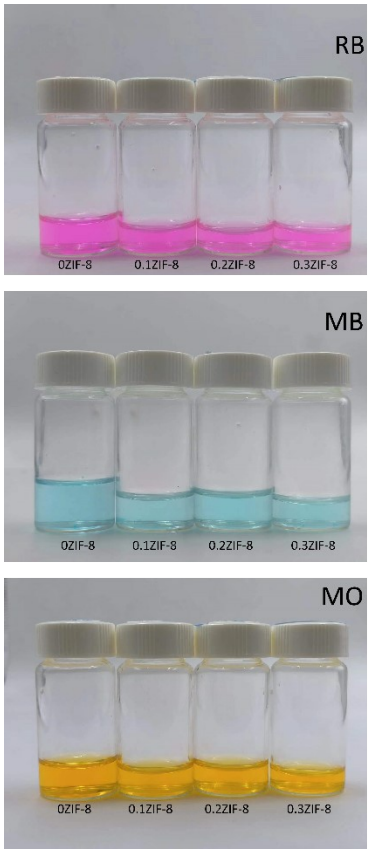

Figure S3. Digital photos of dye solution (RB, MB, and MO) after absorption of HPHG.

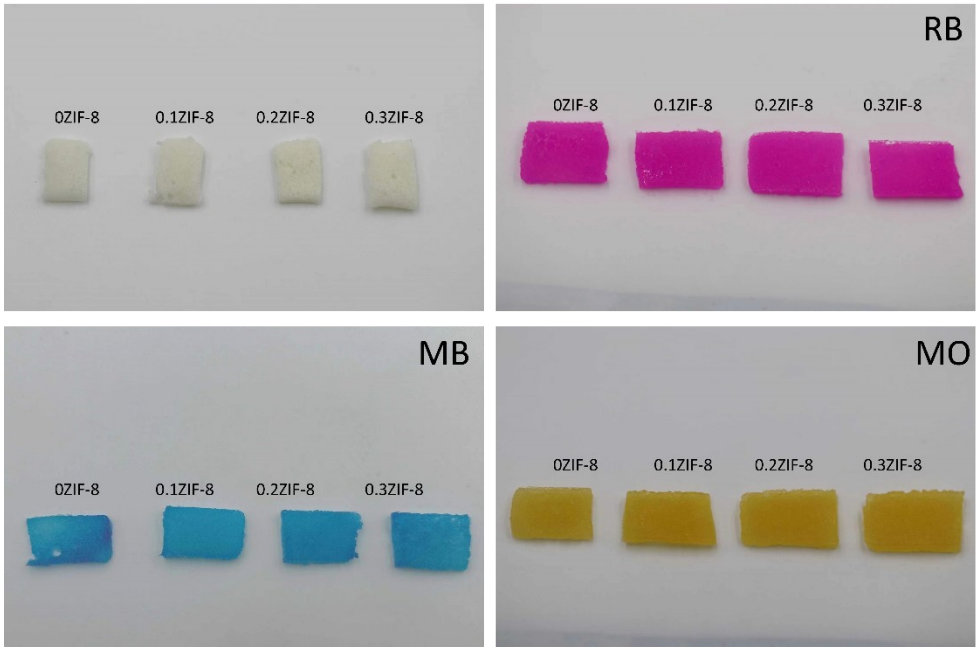

Figure S4. Digital photos of HPHG before and after absorption of different dye.

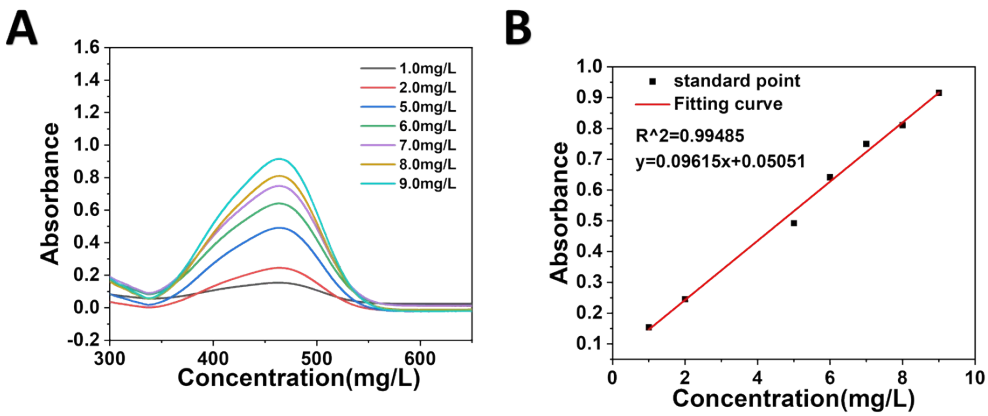

Figure S5. (A) Standard concentration curve of MO. (B) Linear fit curve of MO.

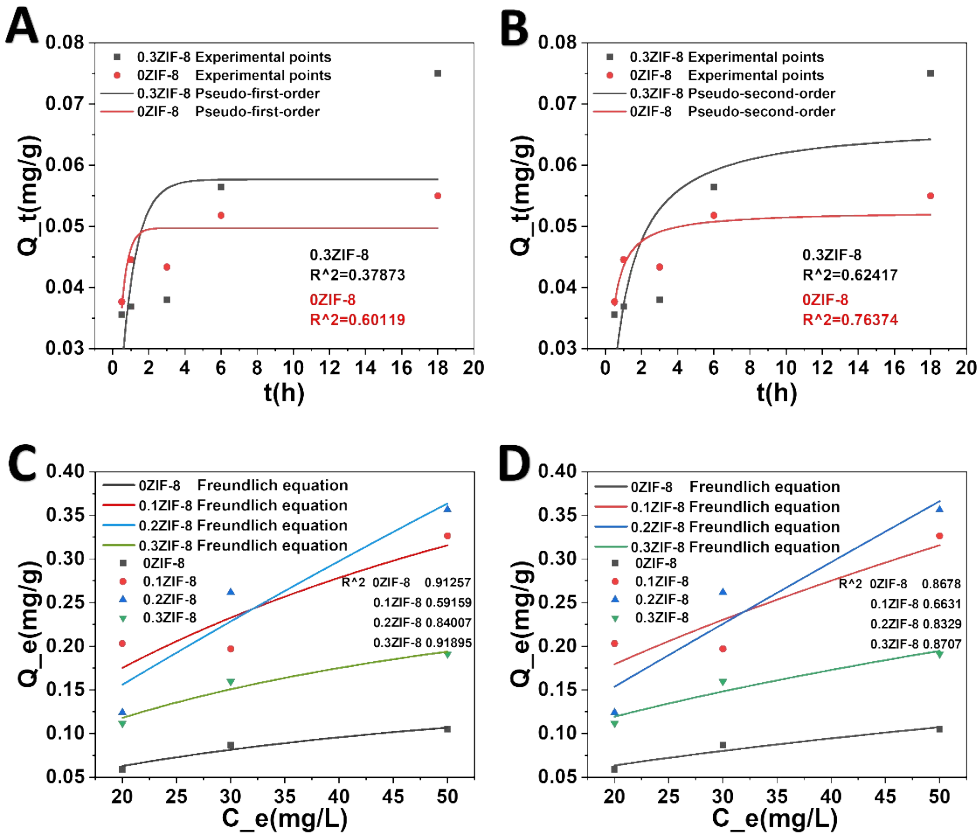

Figure S6. (A) Pseudo-first-order adsorption model and (B) pseudo-second-order adsorption model for the adsorption of MO by HPHG. (C) Langmuir adsorption isotherm and (D) Freundlich adsorption isotherm of MO onto HPHG.

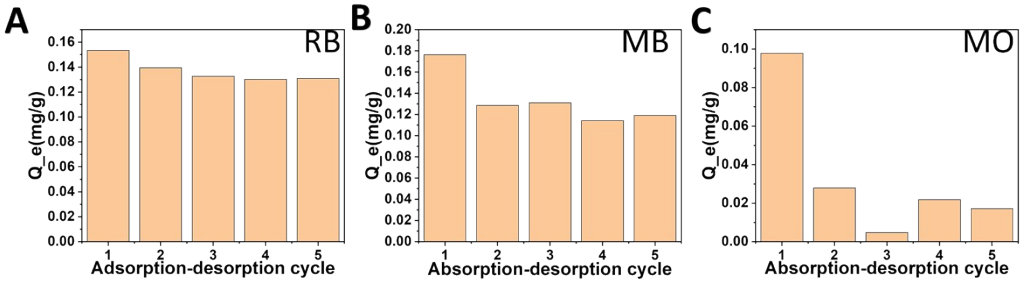

Figure S7. equilibrium absorption capacity of RB, MB, and MO during five adsorption-desorption cycles by HPHG.